

# Surface modification of micromachined silicon filters

YUCHUN WANG\*, MAURO FERRARI†

*Department of Materials Science and Mineral Engineering, University of California at Berkeley, Berkeley, CA 94720, USA*

*E-mail: Yuchun.Wang@amat.com; ferrari@chopin.bme.ohio-state.edu*

Uniform and ultrathin coatings are needed on the surface of micromachined silicon filters in order to manipulate microfluid flow and minimize non specific protein adsorption. This work reports vapor phase deposition of nanometer thick alkylsilanes at atmospheric pressure using nitrogen as a carrier gas. The coatings were characterized with ellipsometry, SEM, AFM, contact angle goniometry, and zeta potential meter. The method is particularly advantageous when it is necessary to coat small channels in microdevices. Micromachined silicon filters were coated with different alkylsilanes and tested with nitrogen gas and a variety of liquids. Interesting flow rate reversal of water versus ethanol was observed when the minimum channel dimension shrank from 74 microns to 1.8 microns. © 2000 Kluwer Academic Publishers

## 1. Introduction

### 1.1. Silicon filters

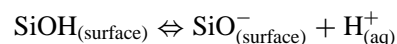
Silicon has been traditionally used for its semiconductor properties in microelectronics. Microfabrication technology, developed for integrated circuits, is now being explored to extend silicon from semiconductor applications to filters and other biomedical microdevices [1–7]. A submicron silicon filter was reported by Kittilsland and Stemme [1] using bulk micromachining and boron doping as etching stop to define channels. Keller and Ferrari [2] filed a patent on the fabrication of silicon filters using surface micromachining, where thin film deposition or growth was utilized to define the channel size. This technology was further developed to make 20-nanometer silicon filters for virus filtration and silicon capsules for immunoisolation [3]. However, such fine structures could not withstand a high pressure and are subject to cracking at about 10 PSI.

To increase the mechanical strength of silicon filters, Tu and Ferrari [4] used surface micromachining to form fine channels and exit holes on one silicon wafer which was thermally bonded to another wafer with entrance holes. This thermally bonded filter can withstand at least 30 PSI, although currently the flow rate is low. In addition to the submicron filters, Brody and Yager *et al.* [5] have studied fluid flow in silicon filters with channel sizes around tens of microns. Their silicon filters were formed by bonding a micromachined silicon wafer with a glass slide so that the flow can be observed through the glass slide; Wilding *et al.* [6] studied biological fluids in straight channels (tens of microns size) for microfluidic manipulations. Overall, the microfabrication technology has enabled the production of silicon

filters with well defined geometry and channel sizes ranging from nanometers to microns with many potential applications. Well defined microchannels would also provide unprecedented experimental tools for the study of microfluids flow.

### 1.2. Surface modification

Silicon surfaces exposed to air or water develop a native oxide layer with surface silanol groups. The silanol groups are ionizable in water:



In fact, silicon surfaces in water are similar to quartz surfaces which have a point of zero charge (PZC) around pH 2 to 3. At pH below 2 the surface is positively charged. At pH above 3 the surface is negatively charged. Thus at neutral pH the silicon surface in water is negatively charged. A charged surface creates a streaming potential in the fluid flow and also promotes protein adsorption. In order to facilitate the flow and minimize protein adsorption, a hydrophilic, neutral, and ultrathin (or monolayer) coating is desired on silicon filters. Previous studies have shown that grafted alcoholic groups can drastically reduce protein adsorption on the surface of contact lenses, glass membranes, and porous silica [8–11]. Therefore alcohol terminated surfaces are highly desirable on silicon filters and other silicon based biomedical devices. As indicated in Fig. 1, we propose to assemble vinyl or glycidoxy groups on silicon filter surface and then to convert them to alcoholic groups.

\* Present Address: Applied Materials, 3111 Coronado Drive, M/S 1512, Santa Clara, CA 95054, USA.

† Present Address: Ohio State University, Biomedical Engineering Center, 270 Bevis Hall, Columbus, OH 43210-1002, USA.

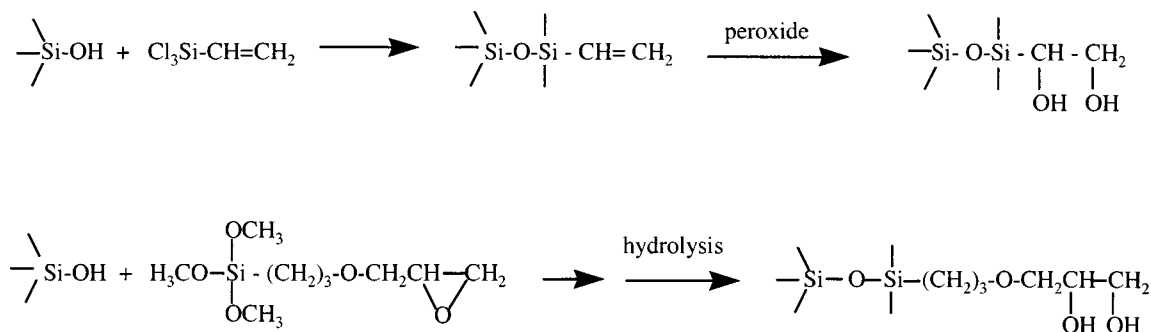


Figure 1 Proposed chemical reactions to assemble alcoholic groups on silicon surface.

Currently the predominant method of surface silanization is to assemble the so-called "monolayer" alkylsilanes onto silicon surfaces in organic solutions [12–14] using alkyltrichlorosilanes (denoted as  $\text{RSiCl}_3$ ) or alkyltrimethoxysilanes (denoted as  $\text{RSi(OCH}_3\text{)}_3$ ), where R is any desired functional group to be introduced into the coating. However, these precursor molecules are sensitive to moisture. The polymerization with trace water in the organic solution or its environment could lead to formation of multilayers and aggregates on silicon surfaces, which would clog up micron-sized channels. In this paper we focus on vapor phase coating of alkyltrichlorosilanes and alkyltrimethoxysilanes on silicon wafers and filters using nitrogen as a carrier gas, as compared with solution coating. The filters were tested with different fluids before and after the vapor phase coating.

Compared with solution coating, the vapor phase coating possesses the following advantages for the surface modification of silicon filters:

1. Easy control of the moisture which affects the coating quality.
2. Ease of vapor access to any irregular channels where the access of liquid would be limited by capillary forces.
3. No toxic solvent is used in vapor phase deposition and contamination is minimized.
4. Incorporation in the standard filter testing protocol, which requires a nitrogen pass-through test. The silanizing reagent can be directly injected into the nitrogen stream following the nitrogen pass-through test in order to assemble a monolayer on the filter surface.

## 2. Experimental procedures

### 2.1. Vapor phase coating and solution coating on silicon wafers

Prior to the surface modification of silicon filters, deposition of alkylsilanes on silicon wafers was explored to understand and control the coating uniformly. Vinyltrichlorosilane (VTS) and 3-Glycidoxypropyltrimethoxysilane (GPTMS) and chlorotrimethylsilane were purchased from Aldrich Chemicals and used as received. For alkylsilane deposition on silicon wafers, semiconductor grade *p*-type test wafers were cut into  $1\text{ cm} \times 2\text{ cm}$  chips and cleaned in 3 : 1 sulfuric acid and 30% hydrogen peroxide (known as piranha) at  $120^\circ\text{C}$  for 10 minutes. The chips were rinsed with deionized water thoroughly.

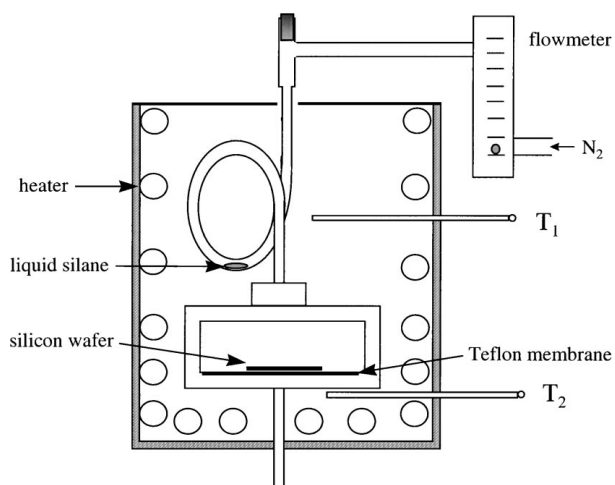


Figure 2 Apparatus of vapor phase deposition to mimic silicon filter surface coating.

Cleaned silicon wafers were dried with nitrogen in a Teflon coating chamber shown in Fig. 2. Nitrogen from a gas cylinder passed through a desiccant tube and a gas flow meter, entered the Teflon chamber, and finally encountered the Teflon membrane at the bottom of the chamber. When the system was stabilized (typically within 20 minutes), the silanizing reagent was injected. The reactant's vapor was picked up by the running nitrogen to coat the silicon surface. The absence of moisture in the chamber allowed only a monolayer to be coated on the surface. Once the surface was saturated with the silanizing reagent the thickness no longer increased.

To compare the results of the vapor phase coating with solution coating, some silicon chips were coated in the silanizing solution using toluene as solvent. In solution coating, the chips were placed in scintillation vials and then toluene (solvent), the silanizing reagent was added to the vials. After mixing, the vials were sealed and stood for a period of time. The chips were rinsed with large amounts of solvent and dried.

### 2.2. Characterization

The coating thickness was measured by ellipsometry (Gaertner Dual Mode Automatic Ellipsometer L116A) at an incidence angle of  $70^\circ$  and wavelength of 6328 Angstroms. Refractive index of 1.46 was assumed for silicon oxide and the organic thin films, with an insignificant effect in the accuracy of the thickness

measurement [12, 15]. The reported thickness is the average difference of the total thickness after coating minus the native oxide thickness (about 1 nm) before coating at 10 different spots for each sample. The standard deviation was typically  $\pm 2$  angstroms for film thickness of one nanometer.

Scanning electron microscopy (SEM) and atomic force microscopy (AFM) were used to check the surface morphology and roughness after the coating. Although nothing was expected to be seen under SEM for an ideal monolayer coating, submicron aggregates or islands were observed by SEM if moisture was not strictly controlled. AFM can give the roughness of the wafer surface as well as morphology. Contact angle goniometry was used to test the wetting on the surface. Water contact angles were measured in this work. XPS (ESCA) was also used to detect whether any residual chlorine was present in VTS coating.

To compare the change of surface charge in water, silicon wafers were ground into a slurry in water. After drying, the silicon powders were coated with VTS or GPTMS under the identical conditions as the coatings of silicon wafers. The zeta potentials of the silicon slurry and the coated silicon powders (particle size around 50 microns) were measured in deionized water.

### 2.3. Vapor phase coating of silicon filters and filter testing

The silicon filters illustrated in Fig. 3 were fabricated in the Microfabrication Lab of UC Berkeley following three separate steps [4]. First, the micron-sized channels and one exit slit are machined into the bottom wafer using lithography, deposition and etching. The minimum dimension of the channels is the channel height. Second, an entrance slit is etched into the top wafer. Finally, the top wafer and the bottom wafer are directly bonded together by thermal annealing in  $N_2$  at  $1000^\circ C$  for 1 or 2 hours. Based on the processing conditions for silicon wafers, silicon filters were coated following the same conditions. Fig. 4 is a diagram of the chamber for silicon filter coating and testing.

After vapor phase coating with the alkylsilanes, the silicon filters were characterized with different fluids: water, 0.2 M NaCl, and ethanol at 3 PSI using the coat-

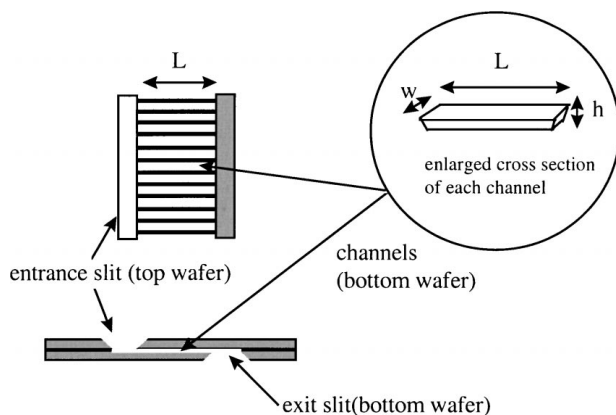


Figure 3 Geometry of silicon filters tested in coating and flow characterization.

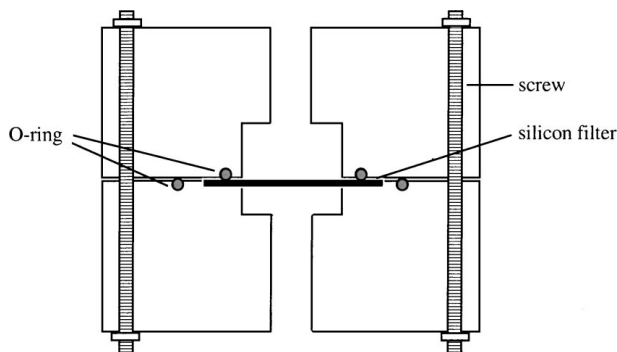


Figure 4 Chamber for silicon filter coating and testing.

ing chamber. The liquid at the exit of the chamber was collected and the mass was continuously recorded on a balance interfaced with a computer. The mass was converted to volume by the known density, and the flow rate was expressed in ml/min.

## 3. Results and discussions

### 3.1. Vapor phase coating with VTS and GPTMS

VTS has a high vapor pressure at room temperature and the vapor phase coating was conducted at room temperature. After the vapor phase coating with VTS, the water contact angle of the wafer was  $80\text{--}90^\circ$ . GPTMS has a lower vapor pressure and is less reactive than VTS. The temperature for GPTMS coating was chosen to be  $90\text{--}100^\circ C$ . The water contact angle after GPTMS coating was around  $60^\circ$ . As seen in Fig. 5, the thickness of both coatings was typically close to 1 nm. As observed by SEM in Fig. 6, no aggregate was found on the wafer surface.

In addition, the samples coated in vapor phase were characterized with Atomic Force Microscopy (AFM). The GPTMS coating shows a smooth surface with rms (root of mean squared) roughness of 0.12 nm, which is in the same roughness range of silicon wafers. AFM micrograph of VTS coating surfaces had rms roughness of 0.32 nm, with some wavy patterns, reflecting different texture of the surface. The coating composition was characterized with XPS. No residual chlorine

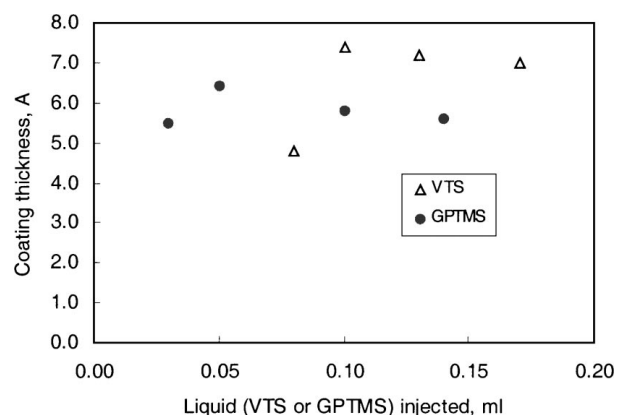


Figure 5 VTS vapor phase coating at  $23^\circ C$  for 2 hours and GPTMS vapor phase coating at  $100^\circ C$  for 2 hours. The coating thickness did not increase with the amount of liquids injected.

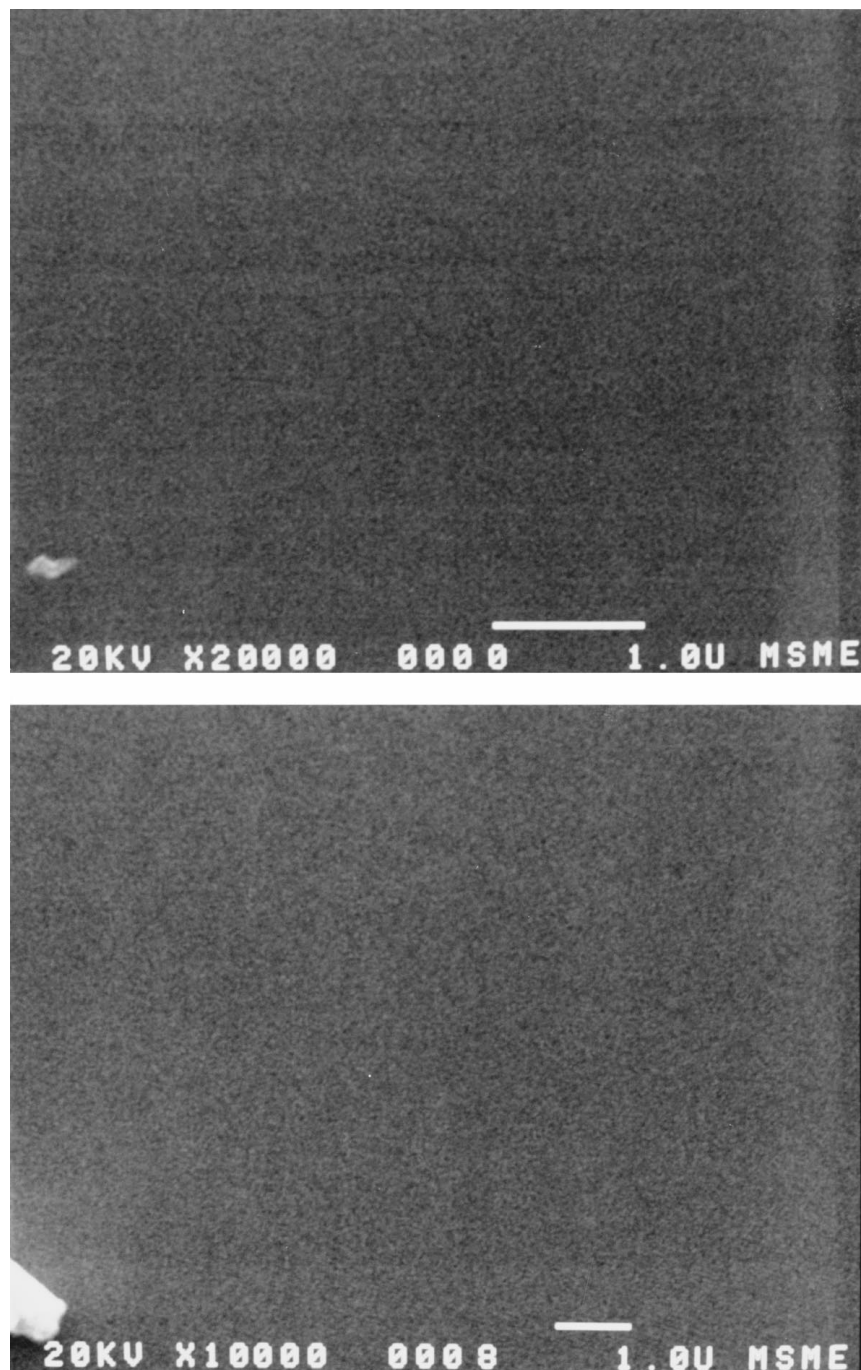


Figure 6 SEM of smooth sample surface after vapor phase coating with VTS (top) and GPTMS (bottom).

was found by XPS on the VTS coating surface, indicating that chlorine was completely removed from the surface as HCl.

### 3.2. Solution coating with vinyltrichlorosilane (VTS)

VTS is very reactive towards both silanol groups and water. Ideally in the absence of moisture, VTS would only react with the silanol groups on the surface of silicon wafers and filters to form a self assembled monolayer. In reality, it is difficult to control the moisture sufficiently effectively that only a monolayer forms. Figs 7 and 8 show that the coating thickness increased with both VTS concentration and reaction time. Fig. 9

shows proposed polymeric reactions in the formation of multilayers and aggregates in the presence of moisture. Both the physical dimensions of the coatings and their increasing thickness indicate that multilayers were formed under such conditions. Although it may be possible to obtain a “monolayer” by using very low concentrations and short contact time, it would be very difficult to control the quality of such a coating.

Water contact angles on wafer in the air after VTS coating were about  $90^\circ$ . The contact angles and coating thickness did not change after immersion in water or dilute  $H_2SO_4$  for a week. A sample with a VTS coating 3.5 nm thick was heated in 1 : 1 mixture of 30%  $H_2O_2$  and concentrated  $H_2SO_4$  at  $80^\circ C$  for 10 minutes, and the contact angle dropped to almost zero but the coating

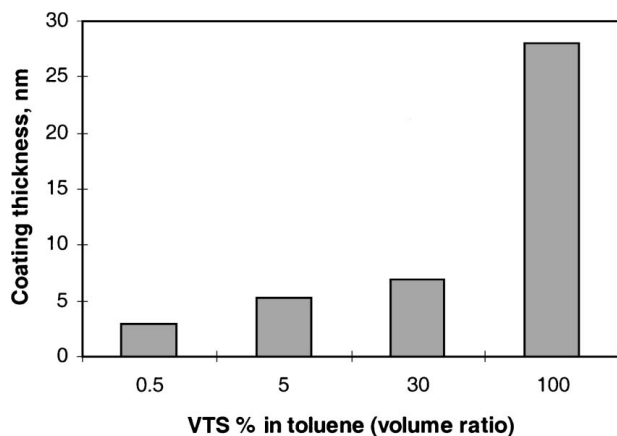


Figure 7 VTS coating thickness increased with VTS concentration. Si wafers were immersed in VTS-toluene solution for 1 hour at 20 °C.

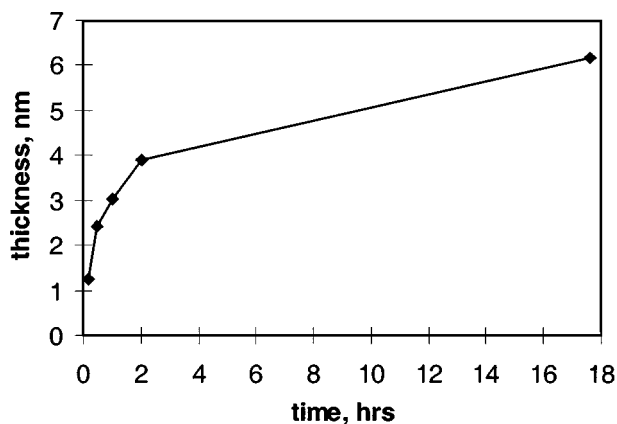


Figure 8 VTS coating thickness increased with reaction time in 0.5% VTS-toluene at 20 °C.

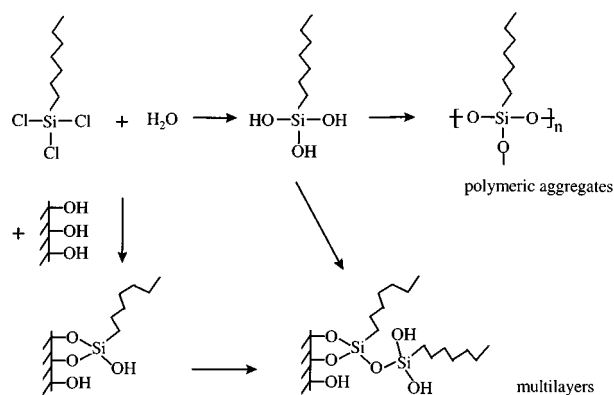


Figure 9 Proposed polymeric reactions in forming polymeric aggregates or multilayers on silicon surface in solution coating when trace water is present in solution.

thickness did not change appreciably (a few angstroms). This indicates that the coating was stable and the vinyl groups were oxidized to hydrophilic groups.

To test the polymerization hypothesis, silicon chips were coated with 5–10% mono-chlorotrimethylsilane in toluene. Since mono-chlorotrimethylsilane has only one chlorine per molecule, it is incapable of polymerization. Indeed the coating thickness was always less than 5 Å with water contact angle in air around 90°, which is indicative of a real monolayer as opposed to multilayers in VTS coating. Similarly, the thickness of

TABLE I Coating of silicon in monochlorovinyl dimethylsilane-toluene solution for 20 hours at 20 °C

% conc. (volume ratio)	coating thickness, Å	water contact angles in air
0.5	1.2 ± 1.6	88°
1.0	4.2 ± 1.7	86°
2.0	4.4 ± 2.6	87°
4.0	2.4 ± 1.4	86°

TABLE II ζ potential of silicon particles in water before and after vapor phase coating. Sample X was silicon slurry by grinding silicon wafer in water, dried at 90 °C for 3 hours. Then sample X was split into two samples, Y and Z. Sample Y was coated in VTS vapor at 23 °C for 2 hours. Sample Z was coated in GPTMS vapor at 97 °C for 2 hours

sample	sample treatment	ζ potential (mV) in water (avg of 10 measurements)
X	silicon slurry (suspension)	-28.0 ± 3.5
Y	coated in VTS vapor at 23 °C	-14.0 ± 2.4
Z	coated in GPTMS vapor at 97 °C	5.0 ± 2.0

mono-chlorovinyl dimethylsilane coating was also below 5 Å, as shown in Table I. This confirms the polymerization mechanism of VTS, leading to multilayers in the presence of traces of moisture. Coated samples were also examined with SEM. Some polymeric sub-micron aggregates are clearly seen in Fig. 10a, while the coating with monochlorosilanes has a smooth surface in Fig. 10b.

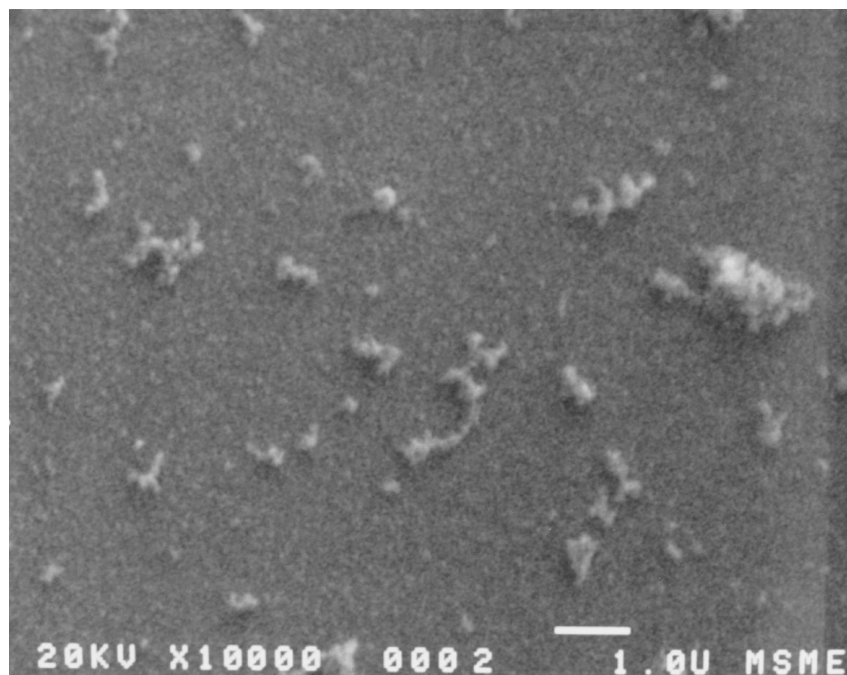
### 3.3. Surface charge before and after the coating

To further probe the surface properties of the coating, silicon wafers were ground into a slurry with deionized water and then coated with VTS and GPTMS. The zeta potential of the fine particles in deionized water after each treatment is listed in Table II. The zeta potential was greatly reduced by VTS vapor phase coating, but the surface was still negatively charged. The residual surface charge, in conjunction with the relative rough surface detected by AFM and coating thickness in Fig. 5, suggests that the coating is more than an ideal monolayer and has residual silanol groups exposed to the air. In contrast, the surface after GPTMS vapor phase coating was almost neutral. This indicates that the surface is better covered by the longer chains in GPTMS than vinyl groups in VTS coating.

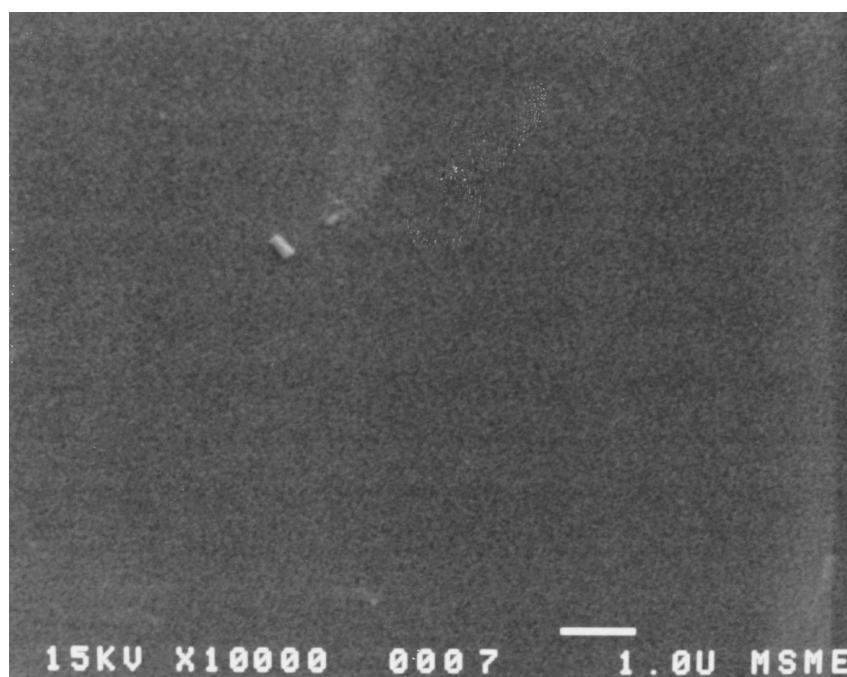
### 3.4. Coating of silicon filters and microfluidics

Silicon filters with channel sizes of microns were coated with alkylsilanes (GPTMS, VTS, and monochlorotrimethylsilane) in vapor phase, and tested with different fluids. Two filters were used and assigned codes F#1, F#2. Their geometry is shown schematically in Fig. 3 and their exact dimensions are listed in Table III.

Filter F#1 was tested for water and 0.2 M NaCl. The flow rate of both water and 0.2 M NaCl was 6.22 ± 0.23 ml/min at 3 Psi with or without coating of GPTMS.



(a)



(b)

Figure 10 SEM of surface coated using (a) 5% vinyltrichlorosilane (VTS)-toluene and (b) 5% monochlorotrimethylsilane in toluene for 1 hour at 20 °C. A particle in (b) was used as a reference for SEM focus.

TABLE III Dimensions of silicon filters used in the coating and testing

	F#1	F#2
channel length ( $L$ ), cm	2.2	2.2
channel width ( $w$ ), $\mu\text{m}$	200	25
channel height ( $h$ ), $\mu\text{m}$	74	1.8
number of channels per filter ( $n$ )	27	20

No change in the flow rate of water was observed. Then, the filter was cooked in piranha for 2 hours in a glass beaker and rinsed with water to recover the surface to silicon oxide. The filter was clamped to the test-

ing chamber, dried by passing nitrogen through the filter, and then coated with VTS by passing VTS vapor through at room temperature. A smooth surface with bluish texture on the filter was seen after the VTS coating, and the water contact angle was around 90°. The bluish texture indicates the coating thickness was close to the visible light wavelength, thus the coating was not a real monolayer due to the residual trace water on the filter surface (the filter was not baked before the coating), which is tolerable in 74 microns channels. After the VTS coating, the flow rate of water, 0.2 M NaCl, and ethanol was measured. Similar to the GPTMS coating, there was no difference between water and 0.2 M NaCl,

both  $6.4 \pm 0.3$  ml/min at 3 Psi. This indicates that electrostatic forces did not play a significant role in 74 microns channels. This observation agrees with the literature [6]. However, the ethanol flow rate was  $5.7 \pm 0.2$  ml/min at 3 Psi. It is interesting that the ratio of flow rate of water to that of ethanol was 1.13, very close to the viscosity ratio of ethanol (1.2 centipoise) to water (1.0 centipoise) at 20 °C. In the classical fluid mechanics, the volume flow rate is inversely proportional to the fluid's viscosity for a fully developed flow between two parallel plates (Hele-Shaw geometry) or in a cylindrical conduct (Hagen-Poiseuille equation). This suggests that in 74 microns channels the flow obeys the classical fluid mechanics. In addition, changing the surface conditions (surface charge and hydrophilicity) in 74 microns channels had negligible effect on the liquid flow rate.

To compare the fluid flow in smaller filters (F#2) with large filters (F#1), water and ethanol were tested through filter F#2, as is shown in Table IV. First the filter F#2 was cooked in piranha for 3 hours at 120 °C to remove any organic contaminants on filter surface, then rinsed with copious water, and immersed in water overnight. The filter was loaded to the test chamber while the filter was still wet with water, followed by the flow test of water and ethanol, respectively. Table IV shows that in 1.8 microns channels the flow rate of ethanol was much higher than that of water and the flow rate ratio was reversed when the channel size shrank from 74 microns to 1.8 microns.

After the fluid test, the filter F#2 was then dried and coated with monochlorotrimethylsilane, which ensures a monolayer coverage and reduced surface charge. The filter was tested first with ethanol because ethanol is easy to permeate into the filter. After the data collection with ethanol, water was loaded to the chamber before ethanol completely drained (this avoids air-water interface inside filter channels). The flow rate of ethanol after the coating, being slightly decreased, was still greater than that of water. The reduced water flow rate in the second batch of test might be resulted from partial clogging by contaminants in water, but the trend of higher flow rate of ethanol than water was repeatable. This higher flow rate of ethanol than that of water was also reported by Kittilsland *et al.* [1] in submi-

TABLE IV Coating of micromachined silicon filters and comparison of flow rate ratios of ethanol over water ( $F_{\text{ethanol}}/F_{\text{water}}$ ) at 3 Psi

Filters	Treatment	$F_{\text{ethanol}}/F_{\text{water}}$
F#1 channel height 74 $\mu\text{m}$	after coating with VTS at 23 °C for 3 hours, tested with water and ethanol, respectively	$0.89 \pm 0.04$
F#2 channel height 1.8 $\mu\text{m}$	after cleaning in piranha at 120 °C for 3 hours, and with water, filter was tested first with water and then with ethanol	$1.76 \pm 0.26$
F#2 channel height 1.8 $\mu\text{m}$	filter was dried and coated with monochlorotrimethylsilane, tested first with ethanol and then with water	$4.27 \pm 1.1$

cron silicon filters. In macro-fluid flow, the flow rate of different liquids is mainly related to viscosity. In micro-fluid flow, the liquid's surface tension and its interaction with the channel surface become predominant as the surface to volume ratio increases. Ethanol has higher viscosity than water, hence lower flow rate than water in large channels. Ethanol, having a lower surface tension and being amphiphilic (hydrophobic with ethyl group and hydrophilic with alcoholic group), may slip along the channel wall more easily than water in small channels.

#### 4. Conclusions

A monolayer or pseudo-monolayer of VTS and GPTMS was deposited on silicon wafers in vapor phase using nitrogen as a carrier gas at atmospheric pressure. The surface charge on silicon in water was blocked or greatly reduced by the coating. Using the vapor phase deposition, different alkylsilanes were deposited on silicon filters with 74 microns channels and 1.8 microns channels. There was no evidence of clogging of the channels in the course of coating. Interesting transition in fluid flow was observed when the minimum channel size shrank from 74 microns to 1.8 microns, indicating that the surface tension of the liquid and interaction of the liquid with the channel surface played a major role in micron-sized channels. This work has demonstrated the deposition of alkylsilanes on silicon wafers and micron-sized silicon filters in vapor phase. Further work is needed to explore the coating of other silanes such as poly(ethylene glycol) silane (biocompatible with low protein adsorption) in micromachined silicon filters.

#### Acknowledgements

We appreciate helpful discussions with Prof. Fiona Doyle and Dr. Tony Hueh. Special thanks go to Larry Glinsky for providing micromachined silicon filters and to Luke Lee, Ron Wilson, and Jinggang Yang for lab assistance.

#### References

1. G. KITTILSLAND and G. STEMME, *Sensors and Actuators A21-A23* (1990) 904.
2. C. G. KELLER and M. FERRARI, US Patent 5 651 900 (1997).
3. T. A. DESAI, W. H. CHU, J. K. TU, G. M. BEATTIE, A. HAYEK and M. FERRARI, *Biotech. and Bioeng.* **57**(1) (1998) 118; T. A. DESAI, W. H. CHU, J. TU, P. SHREWSBURY and M. FERRARI, "Micro and Nanofabricated Electro-Optical-Mechanical Systems for Biomedical and Environmental Application," edited by P. L. Gourley (SPIE, 1997, Vol. 2978) p. 216.
4. J. TU, T. HUEN, R. SZEMA and M. FERRARI, in *SPIE Bios '98 Conference: Micro and Nanofabricated Structures and Devices for Biomedical and Environmental Applications*, San Jose, CA, 1998, Vol. 3258, p. 148. Proceedings of SPIE.
5. J. P. BRODY, P. YAGER, R. E. GOLDSTEIN and R. H. AUSTIN, *Biophysical Journal* **71** (1996) 3430.
6. P. WILDING, J. PFAHLER, H. BAU, J. ZEMEL and L. J. KRICKA, *Clinical Chemistry* **40**(1) (1994) 43.
7. P. C. SIMPSON and R. A. MATHIES, in *SPIE Bios '98 Conference: Micro and Nanofabricated Structures and Devices for Biomedical and Environmental Applications*, San Jose, CA, 1998, Vol. 3258, p. 170. Proceedings of SPIE.

8. G. SCOTT and M. MOWREY-MCKEE, *Current Eye Research* **15**(5) (1996) 461.
9. P. LANGER and R. SCHNABEL, *Chem. Biochem. Eng.* **Q2**(4) (1988) 242.
10. R. SCHNABEL and P. LANGER, *J. Chromatography* **544** (1991) 137.
11. S. H. HO, K. M. GOODING and F. E. REGNIER, *J. Chromatography* **120** (1976) 321.
12. S. R. WASSERMAN, Y. T. TAO and G. M. WHITESIDES, *Langmuir* **5** (1989) 1074.
13. A. ULMAN, *Chemical Reviews* **96** (1996) 1533.
14. R. MABOUDIAN and R. T. HOWE, *J. Vacuum Science and Technology* **B15**(1) (1997) 1.
15. U. JONSSON, G. OLOFSSON, M. MALMQVIST and I. RONNBERG, *Thin Solid Films* **124** (1985) 117.

*Received 2 March 1999  
and accepted 28 February 2000*